PHYSICAL REVIEW B VOLUME 16, NUMBER 2 15 JULY 1977

Electronic band structure of fluorite

J. P. Albert, C. Jouanin, and C. Gout
Centre d'Etudes d'Electronique des Solides, associé au Centre National de la Recherche Scientifique, Université des Sciences et Techniques du Languedoc, Place E. Bataillon, 34060 Montpellier, France
(Received 26 July 1976)

The electronic band structure of CaF_2 is calculated by a mixed tight-binding orthogonalized-plane-wave method. The tight-binding method includes the calculation of three-center terms and the plane waves are then orthogonalized to the occupied levels. The exchange potential is of the Slater form together with a scaling parameter λ adjusted to the gap. The obtained band structure is found to differ significantly with that of previously proposed empirical schemes. Comparison is made with photoemission and optical data and the agreement is good.

I. INTRODUCTION

During the last few years, there has been a great interest in the theoretical study of the electronic structure of the alkali halides. However, in spite of the growing of experimental results about alkaline earth halides, there is very little precise theoretical information on the energy bands in these crystals. This lack of theoretical band calculations can be explained by the fact that the alkaline earth halides have more than two atoms in the unit cell. To date, some experimental material[1-9] has been accumulated on alkaline earth fluorides which requires an interpretation from the stand point of the band structure of these crystals. The purpose of this work is to determine the energy bands of calcium fluoride by a combined tight-binding (TB), orthogonalized-plane-wave (OPW) method.

CaF_2 has been chosen for it can be considered as very representative of the other alkaline earth fluorides (SrF_2, BaF_2) which crystallize in the same structure (the fluorite structure) and whose intrinsic optical spectra posses similar features in the vacuum uv region. In these highly ionic crystals, like in the alkali fluorides, the valence band is principally formed by the outermost p electrons of the F^- ions while the lowest conduction bands are expected to be a mixing of the unfilled s and d electronic states of the cations.

The comparison of the band structure of these crystals with that of the alkali fluorides can therefore provide some insight on the influence of the structure on the band states arising from the same type of ionic levels.

In order to determine the bands proceeding from the filled levels of the ions, we have decided to apply the TB method, as improved by Lafon and Lin.[10] In its present form which incorporates the correct evaluation of three-center terms, this method has proven to be as accurate as other methods and, in addition, does not necessarily incorporate restrictive assumptions about the symmetry of the crystal potential. This technique has proven successful in application to alkali metals,[11] transition-element metals,[12] group-IV crystals,[13] alkali halides,[14,15] and recently CaO.[16]

The only difference between those[14] and our work[15] lies in the fact that we use the TB method to calculate only the valence band, while, in those other works, the whole band structure is calculated by this method. Our basis functions are then formed by the only filled orbitals of the ions. Then, they need not incorporate the excited states which are highly diffuse and thus make the convergence of lattice summations very slow.

The conduction band of CaF_2 is expected to be rather free-electron-like and thus we have used the OPW method. This same approach has been used by many authors in calculating the energy bands of solid-rare[17] gases, alkali halides,[18] and cuprous halides.[19] In our study the plane waves are orthogonalized to the occupied states previously found by the TB method. Hence, the mixing between the occuped orbitals in the crystal is explicity taken into account when calculating the conduction band.

II. CRYSTAL SYMMETRY AND THE MODEL POTENTIAL

The fluorite lattice is shown in Fig. 1. The unit cell includes three ions, one cation chosen as origin, and two anions which are situated at $(\frac{1}{4}a, \frac{1}{4}a, \frac{1}{4}a)$ and $(\frac{3}{4}a, \frac{3}{4}a, \frac{3}{4}a, \frac{3}{4}a$, where a is the lattice constant[20] ($a = 10.323\,62$ a.u. for CaF_2). The space group is O_h^5 and the Bravais lattice is face centered. Accordingly the Brillouin zone is the same as that of the NaCl structure.

Model potential. The crystal potential is composed of contributions from Coulomb interaction and from exchange as

$$V_{cry}(\vec{r}) = V^{C}_{cry}(\vec{r}) + V^{ex}_{cry}(\vec{r}) \quad . \tag{1}$$

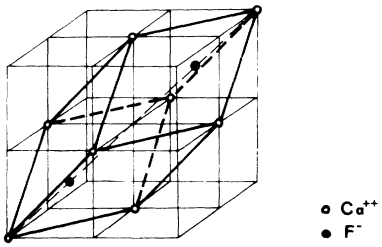

FIG. 1. Unit cell of fluorite crystal.

The Coulomb part has been taken as the superposition of the overlapping Coulomb potentials of the free Ca^{++} and F^- ions. This is based on the assumption that the sum of the free-ion charge densities is a good approximation to the crystal charge density, which is known to be true for highly ionic crystals like this one.[21]

For the exchange part of the potential, we have used the local $\rho^{1/3}$ approximation of Slater[22] together with a multiplicative factor λ. In our work this exchange coefficient λ is treated as an adjustable parameter, $\frac{2}{3} < \lambda < 1$, selected to match some feature of the experimental data (here the gap), although various theoretical prescriptions have been proposed.[22-24]

The Lafon and Lin TB as well as the OPW method require the knowledge of the Fourier coefficients of these potentials, $V^{C}_{\mathrm{cry}}(\vec{K})$ and $V^{\mathrm{ex}}_{\mathrm{cry}}(\vec{K})$.

Using the decomposition of the Coulomb potential over the lattice sites, one obtains without difficulty

$$V^{C}_{\mathrm{cry}}(\vec{K}) = \sum_{\kappa=1}^{3} e^{i\vec{K}\cdot\vec{\tau}_\kappa} V^{C}(K) \ . \tag{2}$$

Here τ_κ specifies the position of atom κ in the unit cell, the sum being on the three atoms (Fig. 1) and $V^{C}_{\kappa}(K)$ is the Fourier transform of the Coulomb potential of the individual free ion

$$V^{C}_{\kappa}(K) = -\frac{8\pi}{\Omega_0 K^2}\left(Z_\kappa - \frac{1}{K}\sum_n a_{n\kappa}\int_0^\infty r\ R^2_{n\kappa}(r) \times \sin(Kr)\,dr\right) . \tag{3}$$

Ω_0 is the volume of the unit cell, Z_κ is the atomic number of ion κ, $a_{n\kappa}$ the occupation number of its nth occupied state, and $R_{n\kappa}$ is the radial part of the atomic orbital for that state. Using the analytical atomic orbitals given by Clementi[25] for the Ca^{++} and F^- ions, these coefficients may then be readily evaluated analytically. The exchange crystal potential is given by

$$V^{\mathrm{ex}}_{\mathrm{cry}}(\vec{r}) = -6\lambda[(3/8\pi)\rho_{\mathrm{cry}}(\vec{r})]^{1/3} \ , \tag{4}$$

where ρ_{cry} is the crystalline charge density and λ an adjustable coefficient. However the calculation of the Fourier coefficients of this potential is tedious. In fact, the approximation of this potential as the superposition of individual atomic terms $-6\lambda[(3/8\pi)\rho_{\mathrm{at}}(r)]^{1/3}$ leads to unreasonable results because of the long tail of these $\rho_{\mathrm{at}}^{1/3}$ terms. The use of a screened potential like the Robinson, Bassani, Knox, and Schrieffer[26] model can remedy this problem. However such an approach has been found not to be valid in our case because the screening is not sufficient, due to the low dielectric constant of CaF_2. We have thus adopted a muffin-tin version of this exchange potential, calculating the spherical average of the crystalline charge density around each atom, performing the integrals of this charge density over atomic spheres of radius half the nearest-neighbor distance, and combining them as in (2). Such a procedure has been widely used and has proven adequate in similar band-structure calculations on ionic crystals.[14] It ensures that the crystal exchange is equal to the free-ion exchange near the ion sites where the wave functions are large. Furthermore, it suppresses the exchange potential in the small charge density regions (between the muffin-tin spheres), where it is known that the Slater approximation overestimates the correlations effects.

This model potential was used to calculate both the valence and core bands and the conduction bands, the exchange scaling parameter λ being adjusted to match the experimental gap of CaF_2.

III. VALENCE AND CORE BANDS CALCULATION

Like in the conventional TB method, the electronic wave function is expanded on Bloch sums of atomic orbitals of the ions within the crystal.

$$\phi^{\vec{k}}_{n\kappa}(\vec{r}) = \frac{1}{\sqrt{N}}\sum_\nu e^{i\vec{k}\cdot(\vec{\tau}_\kappa+\vec{R}_\nu)} u_n(\vec{r}-\vec{\tau}_\kappa-\vec{R}_\nu) \ . \tag{5}$$

Here the sum is carried out over all the lattice vectors $\vec{R}_\nu$ and $u_n(\vec{r}-\vec{\tau}_\kappa-\vec{R}_\nu)$ is the nth free-ion state centered at $\vec{\tau}_\kappa+\vec{R}_\nu$.

The crystalline wave function with energy $E^{\vec{k}}_i$ is thus obtained by solving the well-known eigenvalue problem

$$\underline{H}\underline{C}_i = E^{\vec{k}}_i \underline{S}\underline{C}_i \ , \tag{6}$$

where $\underline{H}$ and $\underline{S}$ are the Hamiltonian and overlap matrices in the ionic Bloch function basis and $\underline{C}_i$ is the ith eigenvector whose elements specify the appropriate linear combination of the ionic Bloch sums corresponding to this ith eigenvalue $E^{\vec{k}}_i$. One is thus led to calculate matrix elements of the form

$$\langle \phi^{\vec{k}}_{n\kappa} | O | \phi^{\vec{k}}_{n'\kappa'} \rangle = \sum_{\nu} e^{i\vec{k}\cdot(\vec{\tau}_{\kappa'}+\vec{R}_{\nu}-\vec{\tau}_{\kappa})} \times \langle u_n(\vec{r}-\vec{\tau}_{\kappa}) | O | u_{n'}(\vec{r}-\vec{\tau}_{\kappa'}-\vec{R}_{\nu}) \rangle , \tag{7}$$

where O is either the kinetic-energy operator for the kinetic-energy integrals, $V_{cry}(\vec{r})$ for the potential energy integrals, or the identity for the overlap integrals.

The kinetic energy and overlap integrals are of two-center type and present no difficulty in evaluating them. In order to avoid the three-center terms appearing in the conventional TB calculation when evaluating the potential-energy integrals, $V_{cry}(\vec{r})$ is expanded in a Fourier series on the reciprocal space:

$$V_{cry}(\vec{r}) = \sum_{\vec{K}} V_{cry}(\vec{K}) \cos(\vec{K}\cdot\vec{r}) . \tag{8}$$

When, as suggested by Chaney *et al.*,[27] the atomic orbitals are developed on a Gaussian basis, the potential-energy integrals consist of linear combinations of terms like

$$\sum_{\vec{K}} V_{cry}(\vec{K}) \int \chi_{\alpha}(\vec{r}-\vec{\tau}_{\kappa}) \cos(\vec{K}\cdot\vec{r}) \chi_{\beta}(\vec{r}-\vec{\tau}_{\kappa'}-\vec{R}_{\nu}) \, d^3r , \tag{9}$$

where χ_{α} and χ_{β} are now Gaussian functions.

The integrals appearing in (9) can then be readily evaluated using analytical formulas derived by Chaney *et al.*[27] and Langlinais *et al.*[12] according to the s, p, or d symmetry of the Gaussians.

In our study, the Bloch sums were constructed on the atomic orbitals of all the occupied states of the free Ca^{++} and F^- ions whose Gaussian-type atomic wave functions have been given us by Salez.[28] However it has been suggested that an increase of variational freedom could be gained when one takes Bloch sums of single Gaussians.[29,16] In fact, for the occupied bands, the energy difference between the two results (Bloch sums of atomic orbitals and of single Gaussians) is far smaller than that due to the uncertainties on the potential, as it can be seen, for example, in Table I of Ref. 16. This shows clearly that the atomic orbitals from a good basis set for the calculation of the valence and core states.

In the calculation of the energy integrals [Eq. (9)], it has been previously noted that the sum on the reciprocal lattice converges very slowly, and that a technique for speeding convergence must be employed. We have applied in that case the procedure previously developed by Chaney *et al.*, which is an Ewald-type decomposition, and we refer to their paper[27] for a detailed account of this technique.

The matrix elements of the different operators are then constructed as in (7); their expression with respect to three center integrals are given in the Appendix. These expressions are, in the fluorite lattice and for the three center case, similar to those derived by Slater and Koster[30] for the two center case in the more conventional cubic lattices.

Owing to the rather high degree of localisation of the ionic orbitals, the sums over the neighboring atoms require very few terms. For instance, the interaction between p F^- orbitals (which are the most extended in space) requires a summation to the third nearest neighbor in order to obtain a convergence of 10^{-3} Ry.

In Fig. 2 we have plotted the computed bands obtained when taking the full Slater exchange potential ($\lambda = 1$). Only the higher bands arising from the $2p$, $2s$ F^- and $3p$, $3s$ Ca^{++} states are shown; the other core states of the ions are much lower and give rise to flat bands which do not interact significantly with those bands.

The valence band structure and more generally that of the bands proceeding from the states of the F^- ion is more complex than that of the alkali fluorides because of the presence of the two inequivalent sites of these ions which creates bonding and antibonding linear combinations which

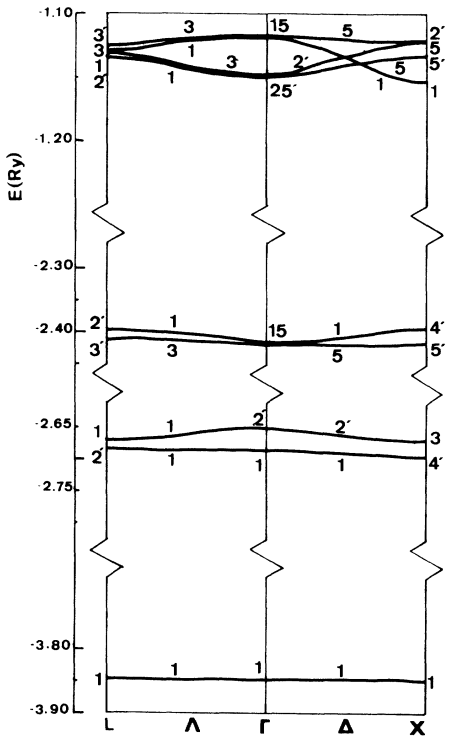

FIG. 2. Occupied bands of CaF_2 with the full Slater exchange.

double the number of levels. Nevertheless, this valence band possesses the same characteristics as that of the alkali fluorides. Its higher branch is practically flat and its width is about the same as that found in other fluorides[14,15] when using the full Slater exchange.

One then finds at about 17 eV lower in energy the bands arising from the $3p$ Ca^{++} states which lie near and interact rather strongly with the $2s$ F^- states. The $3s$ core Ca^{++} states are flat and are situated at about 37 eV from the top of the valence band.

IV. CONDUCTION BANDS

The OPW method is well known and we will give only here a brief outline of the procedure we have used. In this method the basis functions are given by[31]

$$|f_h^{\vec{k}}\rangle = |W_h^{\vec{k}}\rangle - \sum_i \langle\psi_i^{\vec{k}}|W_h^{\vec{k}}\rangle|\psi_i^{\vec{k}}\rangle \ , \tag{10}$$

where $|W_h^{\vec{k}}\rangle$ denotes the normalized plane wave with wave vector $\mathbf{k}+\vec{K}_h$ and the $|\psi_i^{\vec{k}}\rangle$ are all the normalized occupied states previously found by the TB method.

The matrix eigenvalue problem to be solved is then in the same form as in (6), the matrix elements of H and S being now given by

$$\langle f_h^{\vec{k}}|H|f_{h'}^{\vec{k}}\rangle = |\vec{k}+\vec{K}_h|^2\delta_{hh'} + V_{\rm cry}(\vec{K}_{h'}-\vec{K}_h) - \sum_i E_i^{\vec{k}}\langle\psi_i^{\vec{k}}|W_{h'}^{\vec{k}}\rangle\langle W_h^{\vec{k}}|\psi_i^{\vec{k}}\rangle \ , \tag{11}$$

$$\langle f_h^{\vec{k}}|f_{h'}^{\vec{k}}\rangle = \delta_{hh'} - \sum_i \langle\psi_i^{\vec{k}}|W_{h'}^{\vec{k}}\rangle\langle W_h^{\vec{k}}|\psi_i^{\vec{k}}\rangle \ . \tag{12}$$

The $V_{\rm cry}(\vec{K}_{h'}-\vec{K}_h)$ are the Fourier coefficients of the potential previously found and the orthogonalization coefficients $\langle\psi_i^{\vec{k}}|W_h^{\vec{k}}\rangle$ consists of a linear combination of Fourier transform of the atomic orbitals with coefficients $C_{i,n\kappa}$ determined by (6):

$$\langle\psi_i^{\vec{k}}|W_h^{\vec{k}}\rangle = \frac{1}{\sqrt{\Omega_0}}\sum_{n\kappa} C_{i,n\kappa}e^{-i\vec{k}_n\cdot\vec{\tau}_\kappa}\int e^{i(\vec{k}+\vec{K}_n)\cdot\vec{r}}u_n(\vec{r})\,d\vec{r} \ . \tag{13}$$

The bands were obtained with a basis set including 160–180 plane waves. The bottom of the conduction band was found to be the Γ_1 level and thus we have adjusted the theoretical band gap $(\Gamma_{15}-\Gamma_1)$ to its experimental value, 12.1 eV. When this was done a value of 0.795 was found for the scaling exchange parameter λ. This value is to be compared with that found by other workers in ionic solids: 0.75 by Drost *et al.*[14] on LiF, 0.82 by Walch *et al.*[32] on MgO. We have plotted in Fig. 3 the energy bands obtained for such a value of λ. The energies of the levels at the high symmetry points Γ, X, and L are given in Table I.

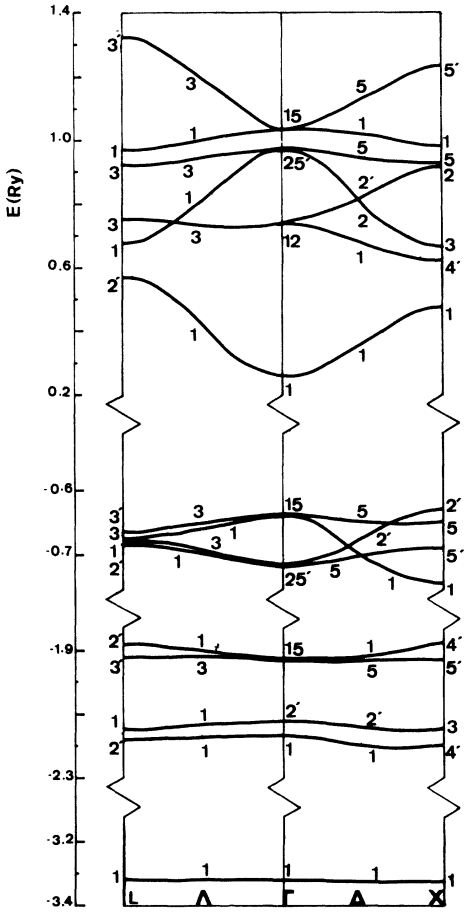

FIG. 3. Energy-band structure of CaF_2 with the exchange scaling parameter $\lambda = 0.795$. Negative energy bands are occupied.

The convergence of the levels with respect to the number of plane waves has been tested at the Γ point because at this point the symmetrization is the most efficient and thus the order of the secular determinants is the lowest, for a given value of $|\vec{k}+\vec{K}_h|$. This convergence is shown in Fig. 4. As can be seen, a basis including 160 plane waves is sufficient to give a well-converged Γ_1 level and thus to fix the gap. The p state Γ_{15} is also well converged with such a basis while the d-type states Γ_{12} and Γ'_{25} would require a greater set. Nevertheless we have verified that the sequence of levels for the lower branches does not suffer by this lack of convergence. In particular enlarging the basis set to 400 or 500 plane waves convinced us that the unusual sequence of levels, Γ_{12} under Γ'_{25}, is not due to this fact.

Before comparing our results with other theoretical and experimental works, let us say a few

TABLE I. Energy of the levels at high symmetry points Γ, X, and L (in Ry). For the occupied bands, the first column lists the ionic states which contribute the most significantly to these levels.

	Γ		X		L	
$1s^+$	1	−292.344	1	−292.344	1	−292.343
$1s^-$	1	−49.008	4′	−49.008	1	−49.008
	2′	−49.007	3	−49.008	2′	−49.008
$2s^+$	1	−30.805	1	−30.806	1	−30.805
$2p^+$	15	−25.127	4′	−25.127	2′	−25.127
			5′	−25.127	3′	−25.126
$3s^+$	1	−3.319	1	−3.319	1	−3.319
$2s^-$	1	−2.169	4′	−2.194	1	−2.150
	2′	−2.124	3	−2.143	2′	−2.180
$3p^+$	15	−1.918	4′	−1.876	2′	−1.885
			5′	−1.921	3′	−1.919
$2p^-$	15	−0.633	1	−0.744	1	−0.681
	25′	−0.712	2′	−0.625	2′	−0.681
			5′	−0.689	3	−0.678
			5	−0.646	3′	−0.664
conduction	1	0.260	1	0.471	1	0.677
	2′	2.125	4′	0.633	2′	0.573
	15	1.032	3	0.676	3	0.757
	25′	0.976	2	0.893	3′	1.337
	12	0.742	2′	2.243		
			5′	1.217		
			5	0.924		

words about the dependence of the bands on the exchange parameter λ. When λ was varied from 1 (Slater exchange) to 0.795 (fit to the experimental gap) the gap varied from 16 to 12.1 eV.

This proceeds from the fact that the (p like) Γ_{15v} level is affected in a different way than the (s like) Γ_{1c} level by exchange. The p-like valence functions have large amplitude in regions of high charge density (near the ions) and are thus far more sensitive to the exchange potential ($\sim\rho^{1/3}$) than the more diffuse s like Γ_{1c} functions. Thus, decreasing exchange shifts the whole band structure to higher energies but the conduction band not as much as the valence band.

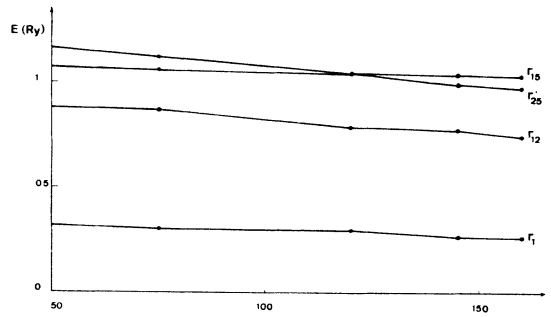

FIG. 4. Energy of conduction levels at Γ vs number of plane waves.

Concerning the occupied bands, as can be seen in comparing Figs. 2 and 3 the essential features of the bands did not change. In particular the interband separation energies and the order of their levels remained the same.

Indeed, the bandwidths, and particularly that of the valence band, are more sensitive and increased significantly when λ was decreased. However the greatest width of the valence band was in the two cases found at X point and was given by the separation

$X_2' - X_1$ (0.5 eV for $\lambda = 1$; 1.6 eV for $\lambda = 0.795$) .

V. COMPARISON WITH OTHER THEORETICAL OR EXPERIMENTAL DATA

Apart from some empirical band schemes proposed by different authors,[3,4,9,33] the work of Starostin[34,35] seems to be the only one which is concerned with a calculation of the electronic structure of CaF_2 from first principles. He calculates the valence band in the TB two-center approximation[34] and subsequently the whole band structure by the OPW method.[35] Our bands are in qualitative agreement with his own, chiefly for the valence and core bands where the sequence of levels and the shape of the bands are quite similar. However his band gap (7.4 eV) and valence bandwidth (9 eV in the TB method, 3.2 eV in the OPW method) are rather different from our results. This seems to be due, either to the two-center approximation or to the lack of convergence in the OPW method for the valence states. The conduction bands, chiefly its lowest branches, are also in good agreement. In particular the same sequence of levels is found at Γ point. Contrary to the alkali halides, Γ_{12} lies lower than Γ_{25}' and Γ_2' is repelled towards higher energies. This is due to the presence of the two inequivalent anions sites in the unit cell which creates linear combinations of occupied s and p orbitals not existing in the NaCl structure and which repel those levels. In the same manner, the d-type X_3 level which was predicted by some authors[3,9] to be an absolute minimum lies even above X_1 because of the existence at this point of a linear combination of occupied s F^- orbitals with the same symmetry. In order to be sure that this is not due to a lack of convergence in our method, we have calculated some key levels of the conduction band structure of CaF_2 and CaO with the same model potential for the Ca^{++} ion.[36]

This potential was obtained so as to give the same band structures of CaO as that found by Mattheiss[37] and Seth *et al.*[16] (where X_3 is found under Γ_1). We then found, that X_3 is repelled above X_1, which convinced us that the sequence of

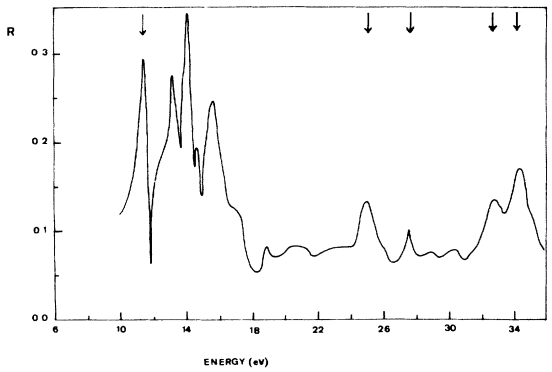

FIG. 5. Reflectance spectra of fluorite at 90 °K (after Rubloff, Ref. 5). Vertical arrows indicate the structures discussed in the text.

levels found in this work is realistic.

Comparison with experimental data. There exists a wealth of experimental data concerning the alkaline earth fluorides and specially calcium fluoride. Concerning the occupied states, photoemission results have been reported by Poole *et al.*[1] and Bremser.[2] The optical constants behavior has also been studied extensively. Reflectance measurements have been made by Tomiki and Miyata[3] near the fundamental optical gap, Stephan *et al.*,[4] Rubloff,[5] and Hayes *et al.*[6] up to 40 eV, and Le Comte *et al.*[7] has made absorption measurements on thin films from 20 to 70 eV. Frandon *et al.*[8] and Lahaye *et al.*[9] have also measured characteristic energy loss up to 140 eV. These different spectra are in good agreement with each other. In Fig. 5 we report the reflectance spectra given by Rubloff.[5] It is composed of a number of fairly strong peaks extending from 11 eV up to 17 eV. Then one finds at about 25 eV a rather large peak, one sharp excitonic peak at 27.7 eV and a fairly broad doublet about 4 eV wide which dominates the high energy part of those spectra around 35 eV.

We report in Table II the experimental and theoretical results concerning the relative positions of the core bands with respect to the valence band. As can be seen our results are in good agreement with the experimental ones. This is surely due to the great care we have taken in order to obtain a good convergence for the potential-energy integrals in the TB part of the calculation. It also tends to prove that the superposition of the individual ionic densities is a good approximation for the crystal charge density and that CaF_2 can be considered as formed of Ca^{++} and F^- ions. Concerning the optical spectra, our purpose is not to make a detailed comparison but to test the validity of our calculation.

The first excitonic pic, which appears in all the experimental spectra, is situated between 11.1 and 11.18 eV, and the gap corresponding to the $\Gamma_{15} \rightarrow \Gamma_1$ transition is evaluated at 12.1 eV. Our theoretical band gap has then been adjusted to this value; that gives a binding energy of about 1 eV for the exciton, in accordance with the values calculated by Tomiki and Miyata[3] and Wiesner *et al.*[38] A detailed interpretation of the following structures up to 17 eV seems to us unrealistic at this stage, first because they are surely related to excited *d* states which are situated a little too high in our calculation and then because, as has been noted by some authors,[39,40] one must be very cautious in assigning peaks to excitonic or band transitions at specific critical points. However, the increasing sharpness and the behavior of these structures when lowering temperature show that this part of the spectrum is dominated by excitonic transitions. Further insight could only be gained by calculating excitonic effects along the lines proposed by Andreoni *et al.*[41] in the cubic rare gases, which lies outside the scope of the present work.

Concerning the large 25-eV peak, it has been attributed[5] to transitions either from the $F^-(2s)$ core level or from the second set of valence bands associated with Γ'_{25}. Our calculation tends to support the second possibility, the $\Gamma'_{25} \rightarrow \Gamma_{15}$ transition being situated at about 24 eV.

The sharp peak situated at 27.7 eV can be iden-

TABLE II. Comparison between the relative positions of core and valence states from theoretical and experimental (photoemission) data. Energies are in electron volts. The zero of energy is taken at the center of the valence band.

Core states	This work $\alpha = 1$	This work $\alpha = 0.795$	TB two-centers approx. (Ref. 34)	Bremser (Ref. 2)	Poole *et al.* (Ref. 1)
$3p^+$	17.4	16.9	19	17.1	17.3
$2s^-$	21	20.1	24.3	21.4	22
$3s^+$	36	37	43.4		36

tified as the core $\Gamma_{15}(p^+) \rightarrow \Gamma_1$ exciton. The corresponding interband transition energy is found at 29.6 eV, which gives for this exciton a binding energy in accordance with that calculated by Hoenerlage *et al.*[2] (1.68 eV).

We then find the rather broad doublet in the 30–35-eV energy range. This doublet is found in calcium compounds (CaF_2, $CaCl_2$, CaI_2,[7] and CaO) and is thus characteristic of the Ca^{++} ion. The $\Gamma_{15}(p^+) \rightarrow \Gamma_{25}(d^+)$, $\Gamma_{15}(p^+) \rightarrow \Gamma_{12}(d^+)$, and $X_5'(p^+) \rightarrow X_3(d^+)$ transitions which could explain these structures are situated in our band structure at about 39, 36, and 35 eV. These theoretical values are a little greater than those predicted by experimental data; this fact is explained by the poor convergence of the OPW method when applied to *d* type states. Transitions from the 2*s* F^- states begin at about 35 eV and can thus explain the weak structures observed on the high-energy side of the doublet.

VI. CONCLUSION

In this study, the electronic band structure of CaF_2 has been calculated with a mixed TB-OPW method. The TB method has been used in the version reformulated by Lafon and Lin which includes the calculation of three-center terms and, in calculating the conduction band, we have used the OPW method, orthogonalizing the plane waves to the states previously found in the TB method.

The model potential was constructed from ionic charge distributions for Ca^{++} and F^-, with an exchange contribution of Slater's form. The bands so obtained were found to disagree with previously proposed empirical schemes. Indeed, concerning the valence bands, the two sets of levels associated with bonding and antibonding orbitals are found to mix strongly all over the Brillouin zone, contrary to what was anticipated in these schemes. It was also shown that the conduction bands cannot be obtained from those of the fcc alkali fluorides. With respect to these crystals, there is an inversion of some levels (Γ_{12} lies below Γ_{25}') and some other levels are repelled upwards. In fact, the minimum of the conduction band is not found to be X_3 as in CaO and some previous empirical schemes but Γ_1. These discrepancies can be explained by the presence of symmetry-type levels in the occupied bands which do not occur in the fcc alkali halides and so perturb significantly the whole band structure.

Our calculated band structure has been shown to compare favorably with experimental data. In particular, the relative positions of the valence and core bands are in good agreement with photoemission results. It has been also shown that the essential features of the optical spectra are satisfactorily interpreted with the obtained band structure. A more detailed interpretation would require a calculation of excitonic effects which lies outside the scope of the present work.

APPENDIX

Matrix elements of the Hamiltonian in the Bloch sums basis for the fluorite structure. There matrix elements are noted $(\mu|\mu')$, where μ and μ' stand for the symmetry type of the wave function (s, x, y, or z). $(E_{\mu\mu'})_{ABC}$ denotes the matrix element of the Hamiltonian (in the three-center calculation) between the atomic orbitals μ centered at $\vec{\tau}_\kappa$ and μ' centered at $\vec{\tau}_{\kappa'} + \vec{R}_\nu$ [see Eq. (7)]. ABC specifies the relative positions of these centers and k_x, k_y, k_z the coordinates of the wave vector. The geometrical factors entering Eq. (7) depend on the symmetry of the shell of neighbors which is summed up and so the expressions were derived according to each symmetry type. Care must be taken that these expressions were derived according to the local symmetry of the anion sites ($\kappa = 2$ and 3) which is only a tetrahedral symmetry (T_d). Concerning the cations interactions one then has to further take into account the effect of inversion.

First class of neighbors $(0, 0, A)$.

$$(s|s) = 2(E_{ss})_{00A}(\cos k_x A + \cos k_y A + \cos k_z A) ,$$

$$(s|x) = 2i(E_{sz})_{00A} \sin k_x A ,$$

$$(x|x) = 2(E_{xx})_{00A}(\cos k_y A + \cos k_z A) + 2(E_{zz})_{00A} \cos k_x A ,$$

$$(x|y) = 2i(E_{xy})_{00A} \sin k_z A .$$

Second class of neighbors $(0, A, A)$.

$$(s|s) = 4(E_{ss})_{0AA} \times (\cos k_y A \cos k_z A + \cos k_x A \cos k_z A + \cos k_x A \cos k_y A) ,$$

$$(s|x) = -4(E_{sx})_{0AA} \sin k_y A \sin k_z A + 4i(E_{sy})_{0AA}(\sin k_x A \cos k_z A + \sin k_x A \cos k_y A) ,$$

$$(x|x) = 4(E_{xx})_{0AA} \cos k_y A \cos k_z A + 4(E_{yy})_{0AA}(\cos k_x A \cos k_y A + \cos k_x A \cos k_z A) ,$$

$$(x|y) = -4(E_{yz})_{0AA} \sin k_x A \sin k_y A + 4i(E_{xy})_{0AA}(\sin k_z A \cos k_y A - \sin k_z A \cos k_x A) .$$

Third class of neighbors (A,A,A).

$$(s|s) = 4(E_{ss})_{AAA}[\cos k_x A \cos k_y A \cos k_z A - i(\sin k_x A \sin k_y A \sin k_z A)] ,$$

$$(s|x) = -4(E_{sx})_{AAA}[\cos k_x A \sin k_y A \sin k_z A - i(\sin k_x A \cos k_y A \cos k_z A)] ,$$

$$(x|x) = 4(E_{xx})_{AAA}[\cos k_x A \cos k_y A \cos k_z A - i(\sin k_x A \sin k_y A \sin k_z A)] ,$$

$$(x|y) = -4(E_{xy})_{AAA}[\cos k_z A \sin k_x A \sin k_y A - i(\sin k_z A \cos k_x A \cos k_y A)] .$$

Fourth class of neighbors (A,A,C).

$$(s|s) = 4(E_{ss})_{AAC}[\cos k_z C \cos k_x A \cos k_y A - i(\sin k_z C \sin k_x A \sin k_y A) + \cos k_y C \cos k_x A \cos k_z A - i(\sin k_y C \sin k_x A \sin k_z A) + \cos k_x C \cos k_y A \cos k_z A - i(\sin k_x C \sin k_y A \sin k_z A)] ,$$

$$(s|x) = 4i(E_{sx})_{AAC}[\cos k_z C \sin k_x A \cos k_y A + i(\sin k_z C \cos k_x A \sin k_y A) + \cos k_y C \sin k_x A \cos k_z A + i(\sin k_y C \cos k_x A \sin k_z A)] + 4(E_{sz})_{AAC}[-\cos k_x C \sin k_y A \sin k_z A + i \sin k_x C \cos k_y A \cos k_z A] ,$$

$$(x|x) = 4(E_{xx})_{AAC}[\cos k_z C \cos k_x A \cos k_y A - i(\sin k_z C \sin k_x A \sin k_y A) + \cos k_y C \cos k_x A \cos k_z A - i(\sin k_y C \sin k_x A \sin k_z A)] + 4(E_{zz})_{AAC}[\cos k_x C \cos k_y A \cos k_z A - i(\sin k_x C \sin k_y A \sin k_z A)] ,$$

$$(x|y) = 4(E_{xy})_{AAC}[-\cos k_z C \sin k_x A \sin k_y A + i \sin k_z C \cos k_x A \cos k_y A] + 4(E_{xz})_{AAC}[\cos k_y C \sin k_z A \cos k_x A + i \sin k_y C \cos k_z A \sin k_x A] + 4i(E_{zx})_{AAC}[\cos k_x C \sin k_z A \cos k_y A + i \sin k_x C \cos k_z A \sin k_y A] .$$

Fifth class of neighbors $(0,B,C)$.

$$(s|s) = 4(E_{ss})[\cos k_y B \cos k_z C + \cos k_y C \cos k_z B + \cos k_x B \cos k_z C + \cos k_x C \cos k_z B + \cos k_x B \cos k_y C + \cos k_x C \cos k_y B] ,$$

$$(s|x) = 4(E_{sx})_{0BC}[-\sin k_y B \sin k_z C - \sin k_y C \sin k_z B] + 4i(E_{sy})_{0BC}[\sin k_x B \cos k_z C + \sin k_x B \cos k_y C] + 4i(E_{sx})_{0BC}[\sin k_x C \cos k_z B + \sin k_x C \cos k_y B] ,$$

$$(x|x) = 4(E_{xx})_{0BC}[\cos k_y B \cos k_z C + \cos k_y C \cos k_z B] + 4(E_{yy})_{0BC}[\cos k_x B \cos k_z C + \cos k_x B \cos k_y C] + 4(E_{zz})_{0BC}[\cos k_x C \cos k_z B + \cos k_x C \cos k_y B] ,$$

$$(x|y) = 4i(E_{xy})_{0BC}[\sin k_z C \cos k_y B] + 4i(E_{yx})_{0BC}[\sin k_z C \cos k_x B] + 4i(E_{xz})_{0BC}[\sin k_z B \cos k_y C] + 4i(E_{zx})_{0BC}[\sin k_z B \cos k_x C] - 4i(E_{yz})_{0BC}[\sin k_x B \sin k_y C] - 4i(E_{zy})_{0BC}[\sin k_x C \sin k_y B] .$$

[1] R. T. Poole, J. Szajman, R. C. G. Leckey, J. C. Jenkins, and J. Liesengang, Phys. Rev. B 12, 5872 (1975).

[2] W. Bremser (unpublished) cited in H. Wiesner and B. Hoenerlaye, Z. Phys. 256, 43 (1972).

[3] T. Tomiki and T. Miyata, J. Phys. Soc. Jpn. 27, 658 (1969).

[4] G. Stephan, Y. le Calvez, J. C. Lemonier, and S. Robin, J. Phys. Chem. Solids 30, 601 (1969).

[5] G. W. Rubloff, Phys. Rev. B 5, 662 (1971).

[6] W. Hayes, A. B. Kunz, and E. E. Koch, J. Phys. C 4, L200 (1971).

[7] A. le Comte and S. Robin, Opt. Acta 19, 203 (1972).

[8] J. Frandon, B. Lahaye, and F. Pradal, Phys. Status Solidi B 53, 565 (1972).

[9] B. Lahaye, thesis (Toulouse, 1973) (unpublished).

[10] E. E. Lafon and C. C. Lin, Phys. Rev. 152, 579 (1966).

[11] W. Y. Ching and J. Callaway, Phys. Rev. B 9, 5115 (1974).

[12] J. Langlinais and J. Callaway, Phys. Rev. B 5, 124 (1971).

[13] R. C. Chaney, C. C. Lin, and E. E. Lafon, Phys. Rev. B 3, 459 (1971).

[14] R. C. Chaney, E. E. Lafon, and C. C. Lin, Phys. Rev. B 4, 2734 (1971); D. M. Drost and J. L. Fry, *ibid.* 5,

684 (1971); N. E. Brener and J. L. Fry, *ibid.* 6, 4016 (1972); N. E. Brener, *ibid.* 7, 1721 (1972).
[15]C. Jouanin, J. P. Albert, and C. Gout, Nuovo Cimento B 28, 483 (1975).
[16]U. Seth and R. Chaney, Phys. Rev. B 12, 5923 (1975).
[17]R. S. Knox and F. Bassani, Phys. Rev. 124, 652 (1961). W. B. Fowler, Phys. Rev. 132, 1591 (1963).
[18]S. Oyama and T. Miyakawa, J. Phys. Soc. Jpn. 21, 868 (1965).
[19]K. S. Song, J. Phys. (Paris) 29, 195 (1967).
[20]R. W. G. Wyckoff, *Crystal Structures* (Interscience, New York, 1975), Vol. 1.
[21]A. Ruuskanen and K. Kurki-Suonio, J. Phys. Soc. Jpn. 34, 715 (1973).
[22]J. C. Slater, Phys. Rev. 81, 385 (1951).
[23]W. Kohn and L. J. Sham, Phys. Rev. 140, A1133 (1965).
[24]R. Gaspar, Acta. Phys. Acad. Sci. Hung. 3, 263 (1954).
[25]E. Clementi, Tables of Atomic Functions (I.B.M. Corp. San José, 1968) (unpublished).
[26]J. E. Robinson, F. Bassani, R. S. Knox, and J. R. Schrieffer, Phys. Rev. Lett. 9, 215 (1962).
[27]R. C. Chaney, T. K. Tung, C. C. Lin, and E. E. Lafon, J.Chem. Phys. 52, 361 (1970).
[28]C. Salez (private communication).
[29]J. E. Simmons, C. C. Lin, D. F. Fouquet, E. E. Lafon, and R. C. Chaney, J. Phys. C 8, 1549 (1975).
[30]J. C. Slater and G. F. Koster, Phys. Rev. 94, 1498 (1954).
[31]T. O. Woodruff, in *Solid State Physics*, edited by F. Seitz and D. Turnbull (Academic, New York,1957), Vol. 4.
[32]P. F. Walch and D. E. Ellis, Phys. Rev. B 8, 5920 (1973).
[33]N. V. Starostin, Fiz. Tverd. Tela 11, 1624 (1969) [Sov. Phys.-Solid State 11, 1317 (1969)].
[34]N. V. Starostin and V. A. Ganin, Fiz. Tverd. Tela 15, 3404 (1973) [Sov. Phys.-Solid State 15, 2265 (1974)].
[35]N. V. Starostin and M. P. Shepilov, Fiz. Tverd. Tela, 17, 822 (1975) [Sov. Phys.-Solid State 17, 523 (1975)].
[36]J. P. Albert, thesis (Montpellier, 1976) (unpublished). J. P. Albert, C. Jouanin, and C. Gout (unpublished).
[37]L. F. Mattheiss, Phys. Rev. B 5, 290 (1972).
[38]H. Wiesner and B. Hoenerlage, Z. Phys. 265, 43 (1972).
[39]S. T. Pantelides, Phys. Rev. B 11, 2391 (1975). A. B. Kunz, Phys. Rev. B 12, 5890 (1975).
[40]K. Kamesrava Rao, T. K. J. Moravec, J. C. Rife, and R. N. Dexter, Phys. Rev. B 12, 5937 (1975).
[41]W. Andreoni, M. Altarelli, and F. Bassani, Phys. Rev. B 11, 2352 (1975).
[42]R. C. Whited and W. C. Walker, Phys. Rev. 188, 1380 (1969).